Experimental Studies of Temperature-Controlled Discharge Characteristics and Calculation of the Heat Generation Rate of NMC Type Battery Cells

A.N. Varyukhin
Electric and Hybrid propulsion systems and aircraft. Central Institute of Aviation Motors (CIAM)
Moscow, Russia

V.S. Zakharchenko
Electric and Hybrid propulsion systems and aircraft. Central Institute of Aviation Motors (CIAM)
Moscow, Russia

A.A. Osika
Electric and Hybrid propulsion systems and aircraft. Central Institute of Aviation Motors (CIAM)
Moscow, Russia

G.S. Ivanov
Electric and Hybrid propulsion systems and aircraft. Central Institute of Aviation Motors (CIAM)
Moscow, Russia

D.V. Zhuravlev
Electric and Hybrid propulsion systems and aircraft. Central Institute of Aviation Motors (CIAM)
Moscow, Russia

I.O. Kiselev
Electric and Hybrid propulsion systems and aircraft. Central Institute of Aviation Motors (CIAM)
Moscow, Russia

A.V. Geliev
Electric and Hybrid propulsion systems and aircraft. Central Institute of Aviation Motors (CIAM)
Moscow, Russia
avgeliev@ciam.ru

A. N. Kim
Electric and Hybrid propulsion systems and aircraft. Central Institute of Aviation Motors (CIAM)
Moscow, Russia

***Abstract* — The results of temperature-controlled discharge tests of NMC type battery cells of standard size 18,650 are presented. A mathematical model of heat generation rate in a battery cell during its discharge is proposed and substantiated in terms of thermodynamics. Based on the model and test results, it is shown that the optimal energy efficiency is the cell discharge mode at a temperature of 55 °C.**

Keywords—battery cell heat generation rate, discharge capacity, temperature-controlled discharge curve

I. INTRODUCTION

Presently, there is a global trend towards toughening of environmental standards imposed on transport systems, including civil aircraft. A possible way to reduce polluting emissions is the use of electric propulsion systems (EPS) based on batteries and fuel cells. E.g., at present, the Pipistrel Alfa Electro [1] electric airplane is serially produced. Its electric motor rotating the propeller is power supplied by batteries during the entire flight. The operation of battery cells which are structural units of a battery pack is accompanied by heat release, which imposes additional restrictions on the conditions of their operation as part of an electric propulsion system of an aircraft. The optimal operating mode of the battery pack, from the point of view of both energy efficiency and safety, requires the development of a battery thermal management system. Its characteristics directly depend on the heat-generating properties of the battery cells.

Currently the Central Institute of Aviation Motors (CIAM) is creating an EPS demonstrator using batteries for a two-seater aircraft with a take-off weight of up to 600 kg. The battery pack consists of NMC type Li-ion cells. In the present study, Sony VTC 6 cells were used. Cost and chemical analysis shows their advantages in terms of specific energy and specific power in comparison with other analogs. The standard size, convenient for practical applications, minimizes the time cycle for manufacturing battery packs consisting of such cells.

A key factor that determines the configuration of the battery thermal management system is the heat generation rate of one cell. For safe and reliable operation of the cells, its temperature must be maintained within an acceptable operating range.

A lot of studies [2]-[8] are devoted to the calculation of the heat generation rate of battery cells, which, in turn, directly or indirectly refer to the pioneering study of Bernardi et al. [9]. The authors of [9] deriving the mathematical expression for the heat generation rate of a battery cell, proceed from the energy balance equation. To calculate the temperature rate of the cell in the most general form, they consider the course of various chemical reactions, the possible occurrence of phase transitions in the cell, enthalpy of mixing, electrical work and heat exchange with the environment. Unfortunately, study [9] contains mathematical inaccuracies that complicate the application of the final mathematical relations. E.g., in [9], in the relation for the heat generation rate of the battery cell, it is not said which values remain unchanged when taking the partial derivative of the open circuit voltage with respect to temperature. Due to the lack of detailed information on the physicochemical and phase transformations occurring in the volume of the battery cell, it is necessary to have a rather general, mathematically substantiated and simple relationship for the heat generation rate of the cell.

The present study is devoted to experimental studies of the temperature-controlled discharge characteristics of Sony VTC 6 battery cells and to the development of a heat generation rate mathematical model based on this data. These results will be the basis for the conceptual design of the battery thermal management system for a light aircraft EPS.

978-1-6654-3941-1 @2021 IEEE

II. Mathematical model of the battery cell heat generation rate during discharge

Let us apply the first law of thermodynamics to the discharge process of a cell (1):

$$\delta Q_{cell} = dH_{cell} + \varepsilon_{cell} dq_{dis}, \quad (1)$$

where δQ_{cell} is the elementary amount of heat transferred to the cell from the environment, J; dH_{cell} is the differential of cell enthalpy, J; ε_{cell} is the cell electromotive force, V; dq_{dis} is the elementary amount of charge passed through the cell (the charge given by the cell or the discharge capacity into the external electric circuit).

In practice, it is convenient to measure the cell discharge capacity in ampere-hours (Ah), and not in coulombs, as is customary in the International System of Units. The assumption about a small change in pressure inside the cell is used in expression (1).

The change in pressure must be taken into account when the cell is operated in an abnormal mode with an unacceptably small residual capacity. In this case, there is a strong heating, boiling or expansion of the electrolyte and, as a result, an increase in pressure.

In this study, only the normal operating mode is considered, which is indicated by the manufacturer in the datasheet. In these conditions, the pressure change can be neglected. Besides, only rechargeable cells with high expected number of charge-discharge cycles are considered. The low cell degradation during the charge-discharge cycle is the basis for the application of the general thermodynamic approach, which presupposes the occurrence of slow reversible (quasi-static) processes. Within the framework of these approximations, the electromotive force of a cell is a function of its state, namely, a function of temperature and ion concentrations in the material of both the negative electrode and the positive electrode.

Let's consider the qualitative principle of cell operation using the example of a lithium-ion battery (Fig. **Ошибка! Источник ссылки не найден.**)

A negative graphite electrode is shown on the left side in Fig. 1. Its layered structure allows lithium ions (black dots in the figure) to easily penetrate into the space between the layers. On the right side the figure shows a lithium manganese spinel, which is a positive electrode and has a porous structure into which lithium ions can also penetrate. Solutions of lithium salts in non-aqueous solvents are used as electrolytes in such batteries.

During battery discharge the lithium ions are deintercalated from the carbon matrix at the negative electrode and then intercalated into the oxide at the positive electrode. When the cell is charged, the above processes run in the opposite direction. Thus the processes of charging and discharging are characterized only by the transfer of lithium ions from one electrode to the other.

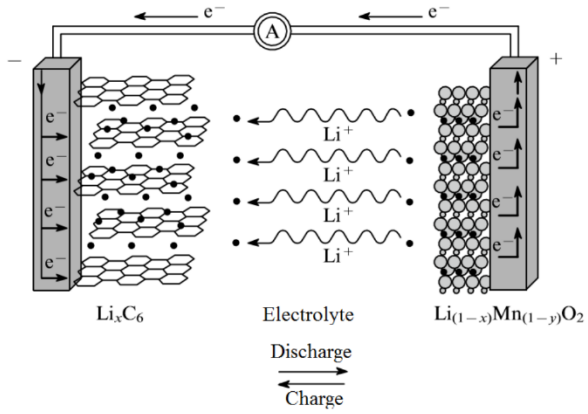

Fig. 1. Li-ion battery circuit

When the cell is connected to an external electrical load the necessary conditions are ensured for the lithium ions to flow from the negative electrode to the positive one through the electrolyte, and electrons flow by the wires of the electrical circuit correspondingly. These processes occur due to the fact that the binding energy of the ion in the material of the positive electrode is higher in modulus than that of the ion in the material of the negative electrode, i.e. the cell discharge process is more favorable in terms of energy. The flow of lithium ions must be artificially limited (breaking the circuit) at a certain closed circuit voltage (CCV), called the cutoff voltage CCV_{coff}. The cutoff voltage of the cell affects its life and is indicated by the manufacturer.

Considering in (1) the quasi-static isothermal flow of an infinitesimal ionic charge dq_{dis} from the negative electrode to the positive one, the electromotive force ε_{cell} can be considered equal to the open circuit voltage (OCV) of the cell. Thus, we conclude that for ε_{cell}, the number of variables which are parameters of the thermodynamic state can be reduced (2):

$$\varepsilon_{cell}(T, q_-, q_+) = OCV(T, q_{dis}), \quad (2)$$

where q_- is the current charge of all ions of the negative electrode, Ah; q_+ is the current charge of all ions of the positive electrode, Ah; T is the absolute temperature, K.

Indeed, the cutoff CCV corresponds to a certain maximum value of the discharge capacity q_{dis}^0, which means that the electromotive force can vary within the following limits (3, 4):

$$\varepsilon_{cell}^{\min}(T, q_-^{\min}, q_+^{\min} + q_{dis}^0) = OCV(T, q_{dis}^0); \quad (3)$$

$$\varepsilon_{cell}^{\max}(T, q_-^{\min} + q_{dis}^0, q_+^{\min}) = OCV(T, 0), \quad (4)$$

where $q_-^{\min}$ is the charge of all ions of the negative electrode of a completely discharged cell, Ah; $q_+^{\min}$ is the charge of all ions of the positive electrode of a fully charged cell, Ah.

The maximum discharge capacity depends on the discharge current and temperature:

$$CCV_{coff} = CCV(T, q_{dis}^0, I). \quad (5)$$

The value of the maximum possible discharge capacity corresponds to the minimum possible discharge current:

$$CCV_{coff} = \lim_{I \to 0} \mathrm{CCV}(T, q_{dis}^{0}(I), I) = OCV(T, q_{dis}^{\max}). \quad (6)$$

Since the total number of ions participating in electrochemical reactions on both electrodes of the cell is invariable if there are no degradation processes. The condition for the constancy of the discharge capacity implies the condition for the constancy of the charge on both the negative and positive electrodes. Thus, the open circuit voltage of the cell is a function of the state of the system, depending on the temperature and the discharge capacity (2).

Considering the quasi-static process of charge flow in the cell and using the Gibbs potential of the cell (Gibbs free energy) together with the second law of thermodynamics, one can obtain the following (7):

$$dG_{cell} = -S_{cell}dT - OCVdq_{dis}, \quad (7)$$

where S_{cell} is the entropy of the cell, J/K; $G_{cell} = H_{cell} - TS_{cell}$ is the Gibbs free energy of the cell (Gibbs potential), J.

In case of isothermal charge flow Δq_{dis} from the negative electrode of the cell to the positive one, the increment of the Gibbs potential can be determined from (7). According to (7), for one mole of ions, one can obtain the following (8):

$$\begin{aligned} \Delta G_{cell}\big|_T = \nu_i \, \Delta\tilde{G}_{cell}\big|_T &= -OCV \cdot n_i e \nu_i N_A \\ \Rightarrow \Delta\tilde{G}_{cell}\big|_T &= -n_i F \cdot OCV \end{aligned}, \quad (8)$$

where ν_i is the the number of moles of ions, mole; n_i is the number of ions produced from one electrochemical reaction of the cell; e is the elementary charge (electron charge), C; N_A is the Avogadro's number, 1/mole; $F = eN_A$ is the Faraday number, C/mole; $\Delta\tilde{G}_{cell}\big|_T$ is the isothermal increment of the Gibbs potential of the cell as a result of its discharge per unit mole of ions, J/mole.

The thermal effect of the chemical reaction is equal to the change in the enthalpy of the reaction except for sign [10]. Since the transfer of charge from the negative electrode of the cell to the positive one is accompanied by useful electrical work produced by electrons as they flow through an external payload, then for the heat generation rate in the cell, the following can be written (9):

$$\frac{dQ_{\mathrm{ht,dis}}}{dt} = -\Delta\tilde{H}_{cell}\frac{d\nu_e}{dt} - I \cdot CCV, \quad (9)$$

where $\frac{d\nu_e}{dt} = \frac{d\nu_i}{dt} = \frac{I}{n_i F}$ is the number of moles of electrons flowing in the circuit per unit time, mole/s; I is the discharge current, A; $\Delta\tilde{H}_{cell}$ is the increment of cell enthalpy per unit mole of ions as a result of its discharge, J/mole; $\frac{dQ_{\mathrm{ht,dis}}}{dt}$ is the thermal power generated in the cell during its discharge, W.

To determine the relationship between the heat generation rate of the cell and its discharge characteristic (the dependence of the CCV on q_{dis} at the discharge current I), the relationship between the Gibbs molar potential (see 8) and the cell molar enthalpy (10) is used:

$$\tilde{G}_{cell} = \tilde{H}_{я} + T\frac{\partial\tilde{G}_{cell}}{\partial T}\bigg|_{q_{dis},P}. \quad (10)$$

Let us consider the heat release from a cell near a small vicinity δT of the temperature of interest to us T_*. By combining (9) and (10), the following is obtained (11):

$$\begin{aligned} \frac{dQ_{\mathrm{ht,dis}}}{dt}\bigg|_{T_* \in (T_*, T_* + \delta T)} = -I\Bigg\{\frac{1}{n_i F}\Bigg[\Delta\tilde{G}_{cell}\big|_{T_* \in (T_*, T_* + \delta T)} - \\ - T\frac{\partial\left(\Delta\tilde{G}_{cell}\big|_{T_* \in (T_*, T_* + \delta T)}\right)}{\partial T}\bigg|_{q_{dis},P}\Bigg] + CCV\Bigg\} \end{aligned}. \quad (11)$$

By tending δT in (11) to zero and using (8), the final expression for the heat generation rate in the cell during an isothermal discharge with a current I is obtained:

$$\begin{aligned} \frac{dQ_{\mathrm{ht,dis}}}{dt}\bigg|_T = I\left[\mathrm{OCV}(T, q_{dis}) - CCV(T, q_{dis}, I)\right] - \\ - IT\frac{\partial OCV(T, q_{dis})}{\partial T}\bigg|_{q_{dis},P} \end{aligned}. \quad (12)$$

Relation (12) allows, when using experimentally obtained temperature-controlled discharge curves $\mathrm{CCV}(T, q_{dis}, I)$ and $\mathrm{OCV}(T, q_{dis})$, determining the heat generation rate of the cell in the entire range of permissible temperatures, discharge currents and discharge capacities.

III. TEMPERATURE-CONTROLLED BATTERY CELL TESTS

The dependence of the closed circuit voltage (CCV) and open circuit voltage (OCV) of the Sony VTC 6 cell on time was measured during the experiments at a constant discharge current and temperature. This study allowed us to determine the dependence of the OCV on the cell temperature (ºC) and the discharge capacity (Ah), as well as the dependence of the CCV on the cell temperature (ºC), the discharge capacity (Ah) and the discharge current (A).

The experiments were conducted in a climatic chamber. Since the air in the chamber has a low heat capacity to ensure thermal stabilization of the cell, the closed loop feedback was implemented using a DS18B20+ temperature sensor [11]. When the cell temperature exceeded the initially set by 1°C, the experiment was stopped until the temperature of the cell in the climatic chamber stabilized to the required temperature with an acceptable error of ± 0.5 °C. After that the experiment continued.

The current was stabilized using a 40xMPN-250 battery test unit manufactured by InEnergy group [12].

Prior to the discharge experiment, the cell was charged from a constant voltage source with V_{sc} =4.2 V. In this case,

the cell charging current decreased until it was below 50 mA. (see fig. 2).

The DS18P20+ digital temperature sensor was attached to the side surface of the cell [11], and the cell itself was placed in the climatic chamber M-70/100-120 KTX [13].

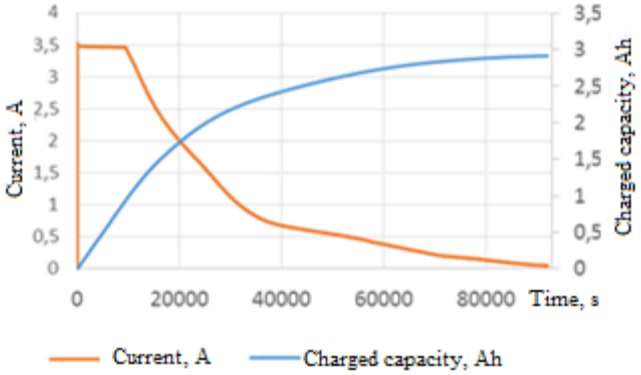

Fig. 2. Sony US18650 VTC6 lithium ion cell charge profile

For each investigated temperature 35°C, 40°C, 45°C, 50°C, 55°C a series of experiments was carried out in which the cell was discharged with a direct current of 9.3 A to a cutoff closed circuit voltage of 2.5 V.

The experiment was carried out in the following sequence:

– connecting the cell to the test bench and placing it in the climatic chamber;
– setting the required temperature in the thermostat;
– setting the discharge current;
– measuring the open circuit voltage at the battery;
– closing the monitoring key and waiting for the current stabilization;
– measuring the closed circuit voltage at the battery;
– key opening;
– waiting for the current to drop to zero and measuring voltage;
– repeating the experiment until the closed circuit voltage reaches the cutoff voltage value of 2.5 V.

The figures below show the graphs of current and voltage values during the cell discharge experiment (Figs. 3-4).

From Figs. 3 and 4 one can conclude that the discharge current stabilization is rapidly converging and allows analyzing the discharge curves of the battery cell.

Based on the experimental data, the dependences of the OCV on the level of charge (discharge capacity) were plotted at different temperatures.

The dependence of the OCV on the discharge capacity at temperatures of 35°C, 40°C, 45°C, 50°C, 55°C is shown in Fig. 5.

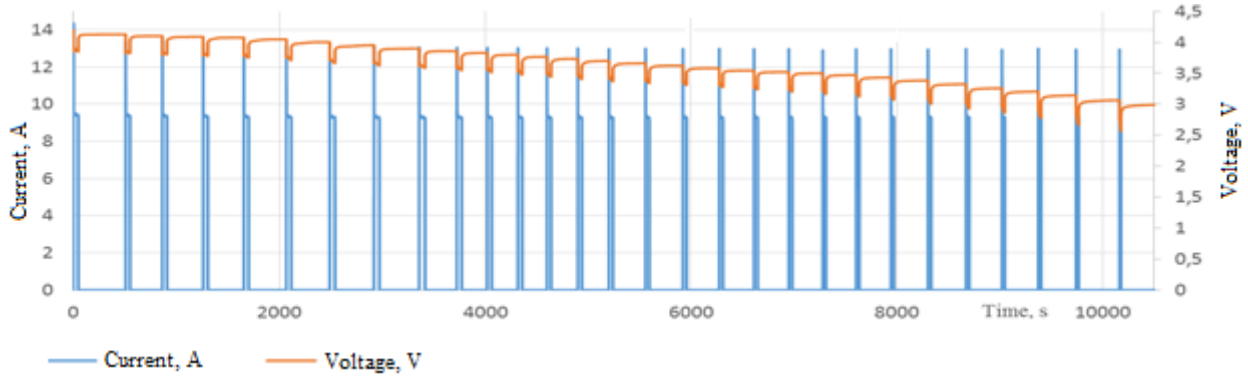

Fig. 3. Voltage and current profile during the experiment (discharge current 9.3 A, temperature 55 ° C)

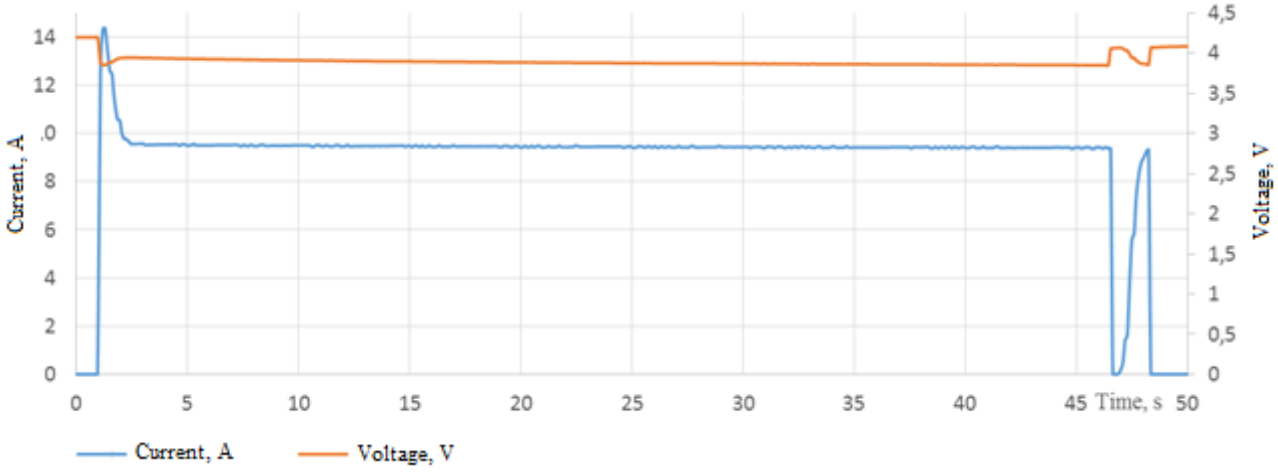

Fig. 4. Voltage and current variations during single impulse discharge (discharge current 9.3 A, temperature 55 ° C)

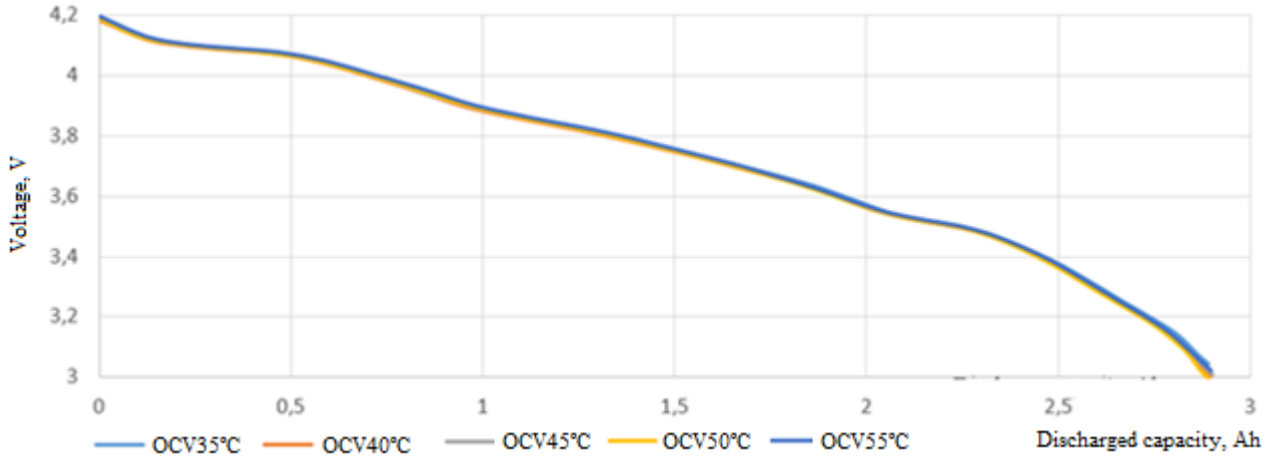

Fig. 5. OCV versus discharge capacity (discharge current 9.3 A) at different temperatures

As follows from Fig. 5, the OCV of a cell weakly depends on temperature at a fixed charge level in the temperature range from 35 to 55 ºC. Such a temperature dependence cannot be explained without large-scale studies concerning the electrochemical processes occurring in the cell and a detailed knowledge of the kinetic, thermophysical, and other characteristics of the structural elements of the cell.

OCV and discharge curves at the discharge current of 7 A at the temperatures of 35°C, 40°C, 45°C, 50°C, 55°C are shown in Figs. 6, 7, 8, 9 and 10, respectively.

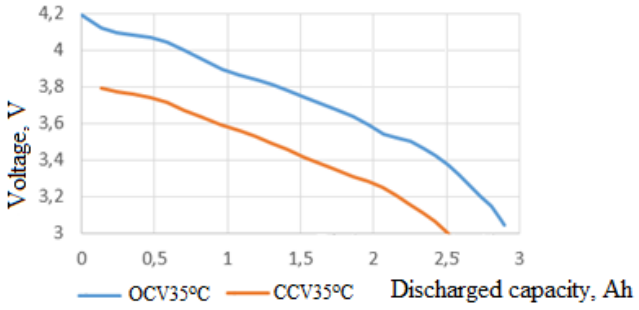

Fig. 6. OCV and discharge curves versus discharge capacity at the current output of 9.3A at the temperature of 35 ºC

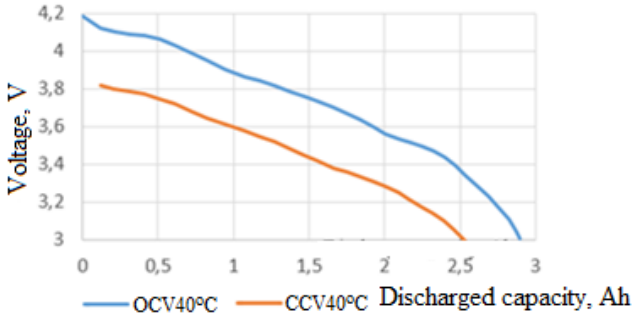

Fig. 7. OCV and discharge curves versus discharge capacity at the current output of 9.3 A at the temperature of 40 ºC

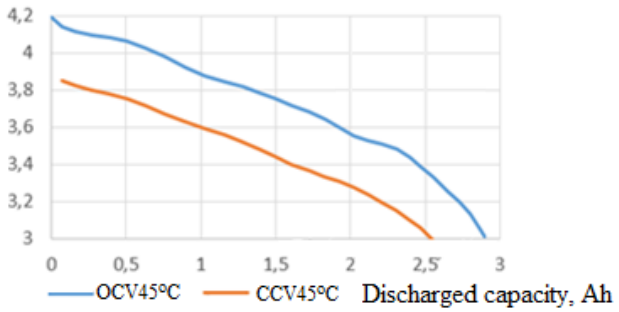

Fig. 8. OCV and discharge curves versus discharge capacity at the current output of 9.3 A at the temperature of 45 ºC

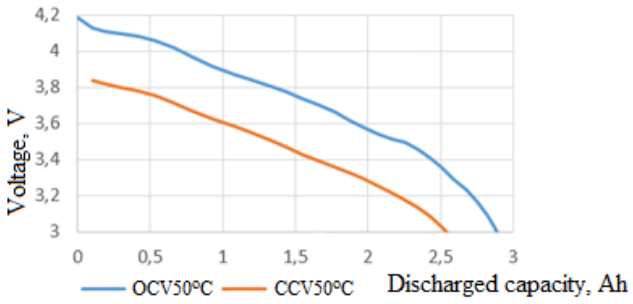

Fig. 9. OCV and discharge curves versus discharge capacity at the current output of 9.3 A at the temperature of 50 ºC

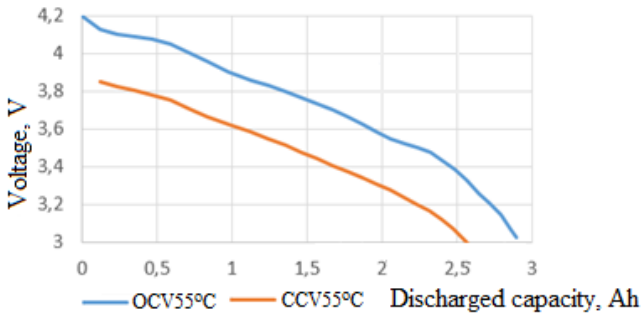

Fig. 10. OCV and discharge curves versus discharge capacity at the current output of 9.3 A at the temperature of 55 ºC

After the circuit opening an increase in OCV is observed depending on time. Fig. 11 shows the dependence of the OCV on time at the capacity of 0.87 Ah immediately after opening

the circuit at the temperature of 35°C. The characteristic cooling time of the Sony VTC 6 battery cell by 0.5 degrees was 385 s, after which the temperature-controlled relative increase in OCV for 54 minutes equaled 0.00258.

In this case, accepting the hypothesis of local thermodynamic equilibrium, relation (12) is also applicable for the unsteady mode.

Discharge curves (see Figs. 6-10) allow determining the heat generation rate of the cells at different temperatures, determined by the expression (12).

In fig. 12, the dependence of the heat generation rate on the discharge capacity is given as an example at the current output of 9.3 A and temperatures of 35, 40, 45, 50, 55 °C.

It follows from Fig. 12 that the heat generation rate decreases monotonically with the temperature increase. An increase in the heat power released by a cell with a decrease in temperature indicates that it is difficult for current-forming electrochemical reactions to occur in it at low temperatures. The optimum temperature for almost all values of the discharge capacity is 55°C (from the selected temperature range).

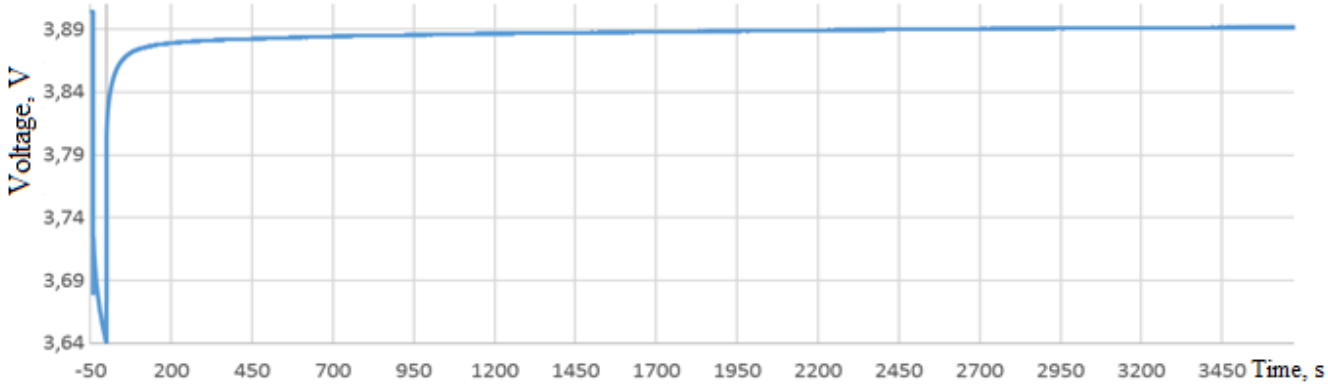

Fig. 11. Voltage-time dependence immediately after opening the circuit at the temperature of 35°C

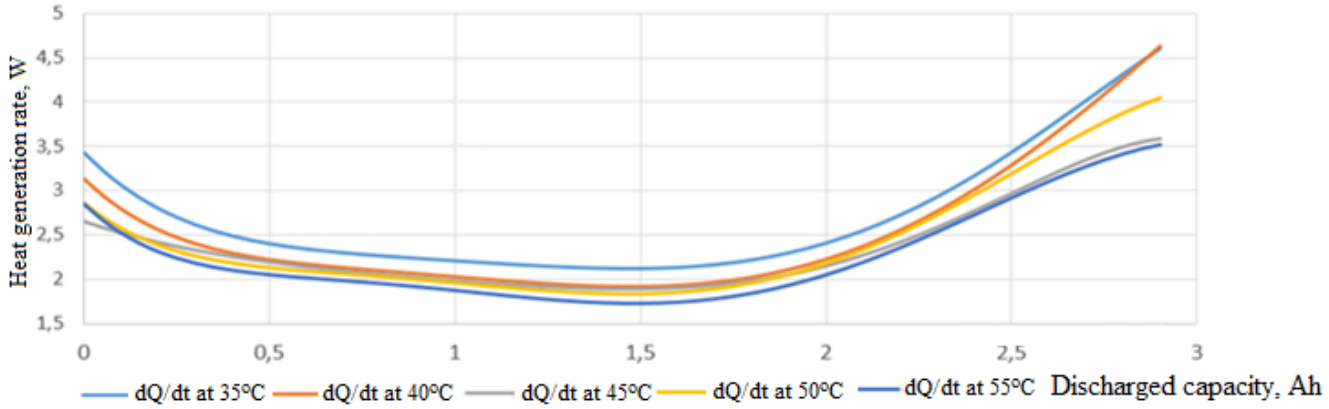

Fig. 12. Heat generation rate of the Sony VTC 6 battery cell versus discharge capacity at the current output of 9.3 A at the temperatures of 35, 40, 45, 50, 55°C

Figure 13 shows the dependence of the contributions to the battery cell heat generation rate of each term of (12) on the discharge capacity at the temperature of 55°C and the current of 9.3 A. For convenience, the first term (13) and the second term (14) contributing to cell heat generation (12) are considered separately:

$$\frac{dQ_1}{dt} = I\left(\mathrm{OCV}(T, q_{dis}) - CCV(I, T, q_{dis})\right) \quad (13)$$

$$\frac{dQ_2}{dt} = -IT\left.\frac{\partial OCV}{\partial T}\right|_{P, q_{dis}} . \quad (14)$$

Figure 13 shows that the maximum relative contribution of the second term (14) to the total thermal power (12) reaches 34% at the given electric charge of 1.5 Ah.

It should be noted that, according to (14), the insufficient accuracy of measuring the OCV can introduce significant uncertainty in calculating the heat generation rate of the battery cell.

When designing lithium-ion battery packs, it is necessary to take into account the balance of generated thermal and electrical power. Figure 14 shows the dependence of the cell electrical power versus the capacity given at temperatures of 35°C, 40°C, 45°C, 50°C, 55°C and a constant current output of 9.3 A.

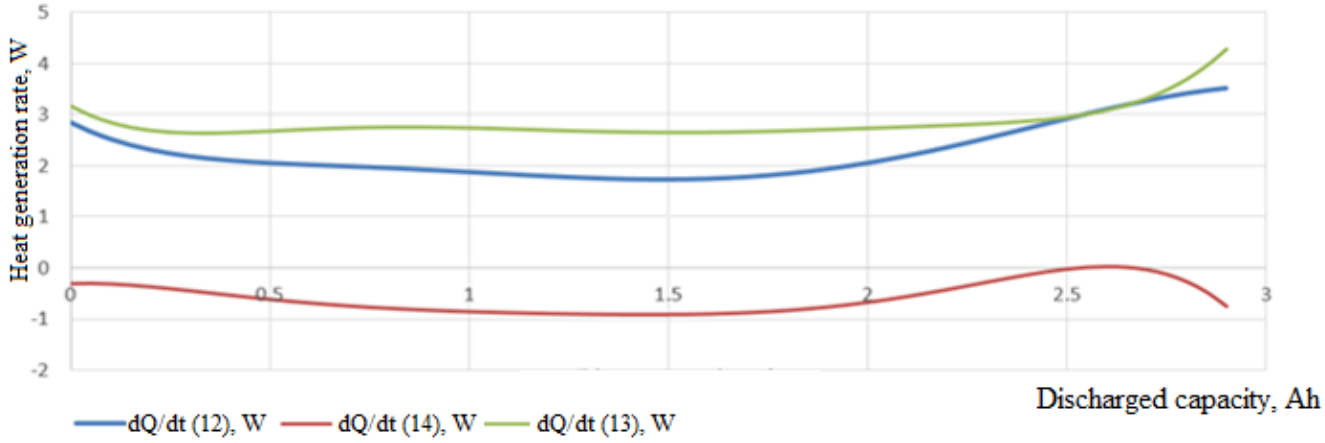

Fig. 13. Dependence of the contributions of each of the terms on the discharge capacity to the heat generation rate of the Sony VTC 6 battery cell at the temperature of 55°C and the current of 9.3 A

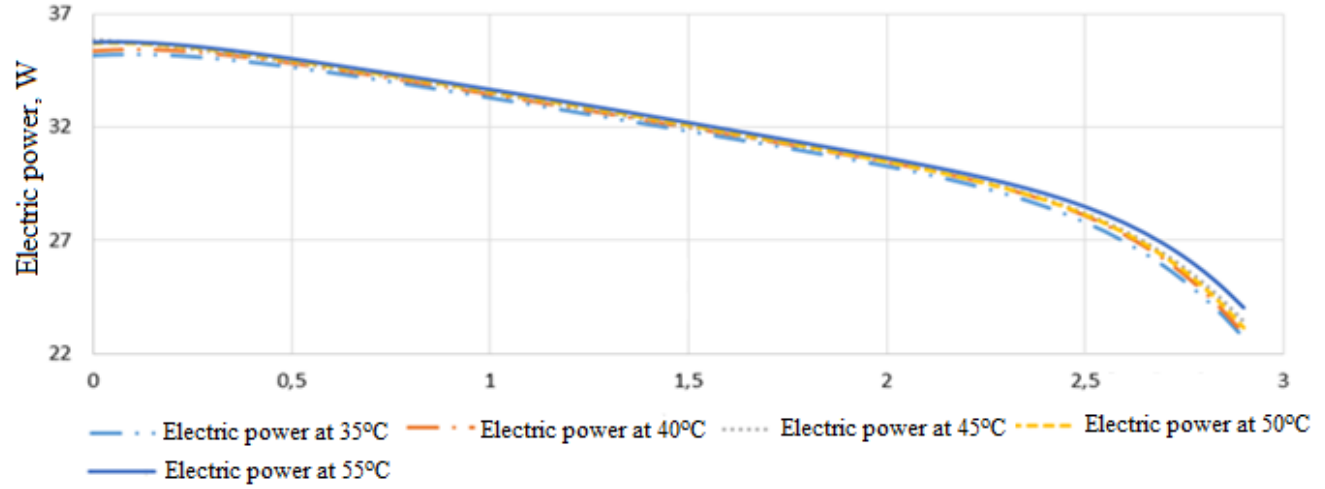

Fig. 14. Electrical power of the Sony VTC 6 battery cell versus discharge capacity at the current output of 9.3 A at the temperatures of 35°C, 40°C, 45°C, 50°C, 55°C

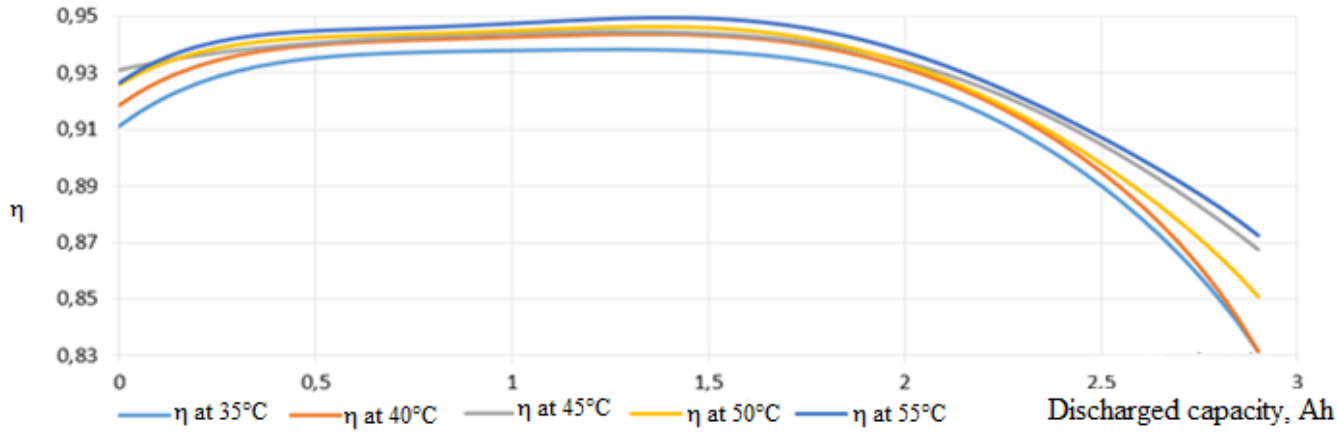

Fig. 15. Cell efficiency versus the discharge capacity at the current output of 9.3 A and temperatures of 35°C, 40°C, 45°C, 50°C, 55°C

At a constant current output and a constant temperature, the electric power decreases monotonically with discharge capacity decrease, which is explained by the CCV decrease.

Let us introduce the battery cell efficiency equal to the ratio of electric power to the sum of electric and thermal powers (15):

$$\eta_{cell}(I,T,q_{dis}) = \frac{I \cdot CCV}{I \cdot CCV + dQ_{ht,dis}/(dt)}. \qquad (15)$$

Fig. 15 shows the cell efficiency versus discharge capacity curves at the temperatures of 35°C, 40°C, 45°C, 50°C, 55°C and the current output of 9.3 A

Experimental discharge and charging characteristics of battery cells are a necessary basis for the conceptual design of a power source based on storage batteries as part of the EPS of promising aircraft.

IV. Conclusion

Temperature controlled discharge tests of lithium-ion NMC type battery cells Sony VTC-6 have been performed. By processing the experimental data, the dependences of the closed and open circuit voltages on the discharge capacity have been obtained in the temperature ranges from 35 °C to 55 °C at various discharge currents.

A thermodynamically valid mathematical model of heat generation rate of a battery cell during its discharge is proposed. It is shown that the cell heat generation rate is determined by the sum of two terms. The first one depends on the output current, the dependence of the OCV and the CCV on the temperature and the discharge capacity. The second one depends on the discharge current, the absolute temperature, the partial derivative of the OCV with respect to temperature at fixed discharge capacity and the pressure inside the battery cell.

The heat generation rate of the Sony VTC 6 battery cell at various temperatures and discharge capacities is calculated based on the proposed mathematical model and the test results. It is shown that the optimal cell discharge temperature in terms of energy efficiency is 55 °C.

References

[1] Pipistrel ALPHA Electro. [Online]. Available: https://www.pipistrel-usa.com/alpha-electro [Date of Access: 14-May-2021].

[2] Y. Abdul-Quadir, T. Laurila, J. Karppinen, K. Jalkanen, K. Vuorilehto, L. Skogström, M. Paulasto-Kröckel, “Heat generation in high power prismatic Li‐ion battery cell with $LiMnNiCoO_2$ cathode material,” International Journal of Energy Research, vol. 38, no. 11, pp. 1424-1437, 2014.

[3] Jong‐Sung Hong, H. Maleki, S. Al Hallaj, L. Redey, J. R. Selman, “Electrochemical‐Calorimetric Studies of Lithium‐Ion Cells,” 1998 Journal of The Electrochemical Society, vol. 145, no. 5, pp. 1489-1501, 1998.

[4] Nur Hazima Faezaa Ismail, Siti Fauziah Toha, Nor Aziah Mohd Azubir, Nizam Hanis Md Ishak, Mohd Khair Hassan, Babul Salam KSM Ibrahim, “Simplified Heat Generation Model for Lithium ion battery used in Electric Vehicle,” in *5th International Conference on Mechatronics (ICOM’13)*, pp. 1-5, 2013.

[5] Shuting Yang, Chen Ling, Yuqian Fan, Yange Yang, Xiaojun Tan, Hongyu Dong, “A Review of Lithium-Ion Battery Thermal Management System Strategies and the Evaluate Criteria,” International Journal of Electrochemical Science, vol. 14, pp. 6077-6107, 2019

[6] W. Lu, I. Belharouak, D. Vissers, K. Amine, “Thermal Study of $Li_{1+x}[Ni_{1/3}Co_{1/3}Mn_{1/3}]_{1-x}O_2$ Using Isothermal Micro-clorimetric Techniques,” Journal of The Electrochemical Society, vol. 153, no. 11, pp. 2147-2151, 2006.

[7] W. Lu, J. Prakash, “Measurements of Heat Generation in a LiÕMesocarbon Microbead Half-Cell,” Journal of The Electrochemical Society, vol. 150, no. 3, pp. 262-266, 2003.

[8] L. Millet, M. Bruch, P. Raab, S. Lux, M. Vetter, “Isothermal Calorimeter Heat Measurements of a 20Ah Lithium Iron Phosphate Battery Cell,” in *12 International Conference on Ecological Vehicles and Renewable Energies*, Monte-Carlo, Monaco, pp.705-711, 11-13 April 2017.

[9] D. Bernardi, E. Pawlikowski, J. Newman, “A general energy balance for battery systems,” Journal of The Electrochemical Society, vol. 132, pp. 5-12, 1985.

[10] Sivukhin, D.V., *General course of physics. Thermodynamics and Molecular Physics*. Fizmatlit, Moscow, 2005.

[11] DS18B20 temperature sensor specification [Online]. Available: http://mypractic.ru/downloads/pdf/DS18B20.pdf [Date of Access: 14-May-2021].

[12] Official website of Inenergy [Online]. Available: http://inenergy.ru [Date of Access: 14-May-2021].

[13] Official site of Grandpribor [Online]. Available: http://grand-pribor.ru//klimaticheskie_kamery/teplo-holod/70-100-120-ktkh.html [Date of Access: 14-May-2021].